# Discovery of a Potent and Orally Bioavailable Benzolactam-Derived Inhibitor of Polo-Like Kinase 1 (MLN0905)

Matthew O. Duffey,* Tricia J. Vos, Ruth Adams, Jennifer Alley, Justin Anthony, Cynthia Barrett, Indu Bharathan, Douglas Bowman, Nancy J. Bump, Ryan Chau, Courtney Cullis, Denise L. Driscoll, Amy Elder, Nancy Forsyth, Jonathan Frazer, Jianping Guo, Luyi Guo, Marc L. Hyer, David Janowick, Bheemashankar Kulkarni, Su-Jen Lai, Kerri Lasky, Gang Li, Jing Li, Debra Liao, Jeremy Little, Bo Peng, Mark G. Qian, Dominic J. Reynolds, Mansoureh Rezaei, Margaret Porter Scott, Todd B. Sells, Vaishali Shinde, Qiuju Judy Shi, Michael D. Sintchak, Francois Soucy, Kevin T. Sprott, Stephen G. Stroud, Michelle Nestor, Irache Visiers, Gabriel Weatherhead, Yingchun Ye, and Natalie D'Amore

Millennium Pharmaceuticals, Inc., 40 Landsdowne Street, Cambridge, Massachusetts 02139, United States

Ⓢ Supporting Information

ABSTRACT: This article describes the discovery of a series of potent inhibitors of Polo-like kinase 1 (PLK1). Optimization of this benzolactam-derived chemical series produced an orally bioavailable inhibitor of PLK1 (**12c**, MLN0905). In vivo pharmacokinetic–pharmacodynamic experiments demonstrated prolonged mitotic arrest after oral administration of **12c** to tumor bearing nude mice. A subsequent efficacy study in nude mice achieved tumor growth inhibition or regression in a human colon tumor (HT29) xenograft model.
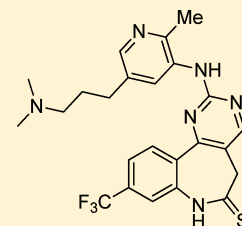
■ INTRODUCTION

Polo-like kinase 1 (PLK1) is a serine/threonine protein kinase that plays a key role in cell cycle control. PLK1 controls entry into and progression through mitosis at multiple stages by regulation of centrosome maturation, activation of initiating factors, degradation of inhibitory components, chromosome condensation, and exit from mitosis.[1] PLK1 has been reported to be overexpressed in numerous cancers such as melanoma, prostate, ovarian, colorectal, pancreatic, non-small-cell lung, esophageal, endometrial, glioma, squamous cell carcinoma of the head and neck, and non-Hodgkins lymphoma.[2] Increased levels of PLK1 expression are additionally correlated with poor prognosis and survival.[2b,3] Overexpression of this kinase transforms cells, rendering them oncogenic such that they acquire the ability to form tumors in mice.[4] PLK1 protein levels are also elevated in tumor relative to normal cell lines in culture. Down-regulation of PLK1 protein expression by RNA interference in tumor cell lines results in a reduction of cell proliferation, mitotic arrest at prometaphase, and rapid progression into apoptosis.[5] This effect was not observed in normal cell lines.[6] Moreover, down-regulation of PLK1 by short hairpin expression in mice with human xenografts reduced tumor growth to 18% of that observed for a control shRNA.[7] Its key role in mitotic progression, its overexpression in a wide range of malignancies, and the antiproliferative effect observed upon its depletion, underscore the merits of evaluating PLK1 as an anticancer target. Indeed, a number of PLK1 inhibitors have advanced into clinical development.[8]

As such, efforts were initiated to identify a small molecule PLK1 inhibitor with drug-like properties. We identified 1 (Figure 1) after progression of our corporate compound library through a PLK1 flash plate-based high-throughput screen.
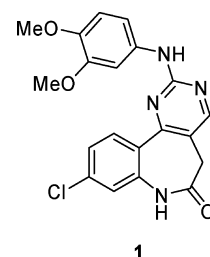
1
PLK1 IC$_{50}$: 31 nM
Cell viability (HT29) LD$_{50}$: 3,300 nM
Solubility (pH=6.8): 11 ug/mL

Figure 1. PLK1 screening hit.

Compound **1** demonstrated good inhibition of the PLK1 enzyme but suffered from suboptimal characteristics including modest cell-based activity and low solubility. Our goals were first and foremost to improve enzyme potency and understand the SAR of PLK1 inhibition. Secondarily, we hoped to create inhibitors of PLK1 that would possess good cellular activity as well as improved physicochemical properties (i.e., solubility).[9] Ultimately, we hoped to identify selective inhibitors that would have adequate in vivo properties to achieve a desirable
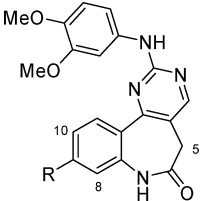
pharmacodynamic response resulting in tumor growth inhibition.

RESULTS AND DISCUSSION

Initial investigation into SAR began with substitution of the benzolactam core. A series of analogues that focused on modification at the C-8, C-10, and C-5 sites of the benzolactam resulted in a decrease in enzyme potency (data not shown). Modification at the C-9 position was tolerated, however (Table 1).

Table 1. SAR of 9-Position on the Benzolactam Core[a]

	R	PLK1 IC$_{50}$ (nM)
1	9-Cl	31 ± 10
5a	9-I	10 ± 2
5b	9-CF$_3$	18
5c	9-H	450 ± 80
5d	9-F	200
5e	9-Me	65 ± 13
5f	9-CN	83
5g	9-Et	31 ± 6

[a]Standard deviations are reported for $N \geq 3$. Otherwise IC$_{50}$ values are mean values of two determinations.

Chloro was replaced with several other small functional groups, and potency against PLK1 was retained. The dechlorinated analogue (5c), however, was significantly less potent. Thus, it

became clear that modification of the benzolactam core was tolerated at the C-9 position, and substitution at this carbon was essential for enzyme potency. However, the series still suffered from a lack of cell potency and poor solubility (data not shown).

Scheme 1 details the synthetic route used for construction of the benzolactam core. In a straightforward manner, aminoesters (2) substituted at C-3 of the phenyl ring were converted to their corresponding 7-membered benzolactams (3). The 3-step sequence began with addition of 3-(carbomethoxy)propionyl chloride to form the amide intermediate. Then, a Dieckmann condensation followed by decarboxylation achieved by refluxing in DMSO/H$_2$O provided 3. The benzolactam was next transformed to the corresponding enamine 4 by heating in the presence of DMF-DMA. A subsequent base promoted condensation with *N*-(3,4-dimethoxyphenyl)guanidine provided aminopyrimidine analogues of general structure 5. For the syntheses of analogues that required further chemical manipulation, the requisite iodinated analogues of 3 (R = I) or 5 (R = I) were transformed to the desired final compounds (see Supporting Information for further details).

In addition to understanding SAR and improving enzyme potency, we also sought to improve the cell activity and solubility of this chemical series. As we were unable to achieve these goals by modification of the benzolactam core, we took aim at other regions of the scaffold. Our strategy focused on creating analogues that varied substitution on the upper aryl ring while keeping chloro constant at the 9-position of the benzolactam core.[10] Appropriately substituted anilines (6) were converted to the corresponding guanidines (7) by one of two methods (Scheme 2). Either the addition of *N,N'*-Di-BOC-*S*-methylisothiourea followed by removal of the BOC protecting groups or the addition of cyanamide in the presence of nitric acid was employed. Condensation of the guanidine with

Scheme 1. General Synthetic Scheme for the Synthesis of Benzolactam Analogues
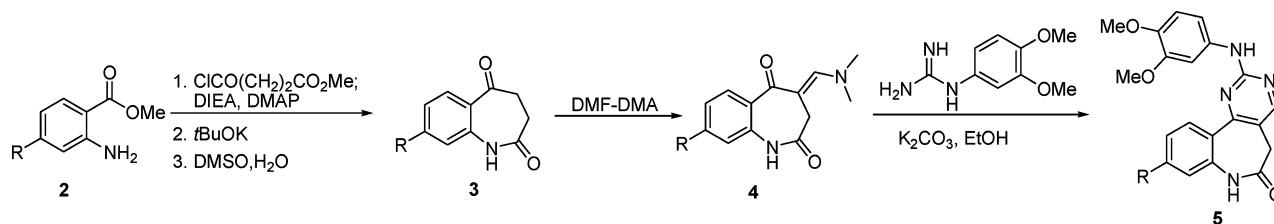
Scheme 2. General Synthetic Scheme for the Synthesis of Analogues in Table 2
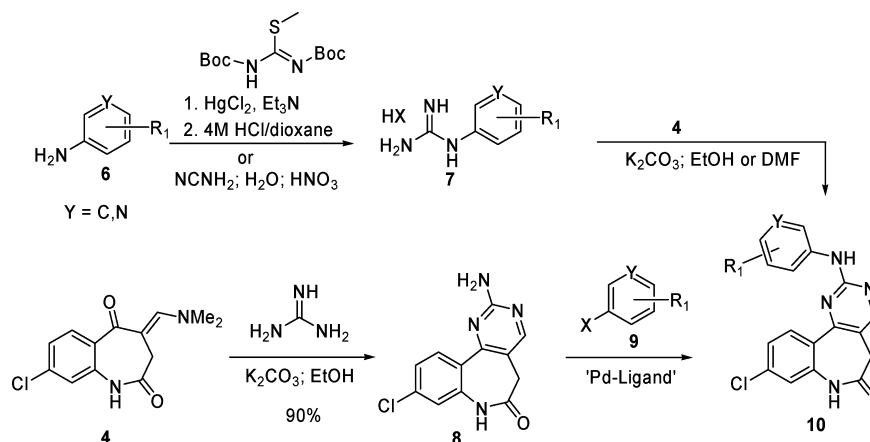
intermediate **4** (R = Cl) allowed generation of analogues of general structure **10**. If the appropriate aniline was not available or easily constructed, then condensation of **4** (R = Cl) with guanidine was employed to provide amino pyrimidine **8**. A Buchwald-type coupling[11] with an appropriate aryl halide (**9**) was then utilized to complete the synthesis and also furnish analogues of general structure **10**.

The compounds in Table 2 were prepared by these methods. Cell activities of analogues were measured in a cell viability assay (HT29) and in a mitotic index assay (MIA).[12] In addition, we developed a Cdc25C-T96 cell-based assay as a direct readout of PLK1 inhibition. Threonine-96 on Cdc25C is a specific phosphorylation site for PLK1.[13] Readout for the assay reported the decrease in the levels of phosphorylated Cdc25C-T96 in treated versus untreated cells.

Analysis of the SAR of the prepared structures showed that systematic removal and repositioning of the methoxy groups on the phenyl ring resulted in analogues with either decreased enzyme potency or decreased cell activity, or both (**10a−10d**). Substitution of the phenyl ring with carboxylic acid groups also decreased cell activity (**10e**, **10f**). A variety of analogues was also constructed to evaluate substitution at the *para* position (C-4′) on the phenyl ring. Introduction of iodide at this site produced a loss of cell activity (**10g**) while installation of amines generally improved solubility but decreased enzyme potency (**10h**, **10i**). Amides at C-4′ gave mixed results (**10j**, **10k**). Although cyclopentyl amide (**10k**) provided increases in enzyme and cell potency, it was poorly soluble. A sulfonamide produced a significant decrease in enzyme potency (**10l**) as did the methylmorpholinoamide substituted at the *meta* position (C-3′) (**10m**). However, when the 3-dimethylaminopropyl group was installed at C-3′, a significant increase in cell activity and solubility was realized while maintaining enzyme potency (**10n**). Further investigation at the C-3′ position revealed that a variety of alkylamino groups decreased enzyme potency (**10o−q**), although acyclic alkylamines gave good solubility (**10p**, **10q**). Additionally, morpholine at C-3′ produced a decrease in enzyme and cell activity (**10r**). From these investigations, **10n** was identified as an important analogue. It exhibited significant improvements in both cellular activity and solubility compared to **1**.

Further optimization of the scaffold led to conversion of the amide of **10n** to its corresponding thioamide by use of phosphorus pentasulfide (Lawesson's reagent could also be used) (Scheme 3). The newly constructed analogue (**11a**) achieved an increase in potency against PLK1 and a significant boost in cell potency over any compound that had been synthesized to date in this chemical series. However, while the thioamide offered an improvement in potency, it also resulted in decreased solubility.

Having achieved a significant increase in cell activity versus the original HTS hit (**1**), we next focused on attaining selectivity over related kinases. To accomplish this, we focused on further chemical manipulation of the upper phenyl ring. Compounds were constructed by making use of the general method outlined in Scheme 2, followed by the thioamide formation detailed in Scheme 3. We found that substitution at C-6′ of the phenyl ring generally resulted in increased selectivity for PLK1 over a small internally available panel of kinases (Table 3). As the steric bulk of the substituent at C-6′ was increased, the selectivity for PLK1 over the kinase panel also increased (**11a−11g**). When R = H (**11a**), little to no selectivity was observed. However, when trifluoromethyl (**11f**)

or *i*-propyl (**11g**) reside at C-6′, a high degree of selectivity for PLK1 was achieved. At the same time, we also observed a slight decrease in cell activity as the steric bulk was increased.

Substitution at other sites on the phenyl ring was also investigated (Table 3). Installation of chloro at C-5′ produced a compound (**11h**) that was equipotent with **11a** but not selective for PLK1 over PLK3. It was also poorly soluble. Introduction of various functionalities at C-4′ of the phenyl ring also provided a series of analogues that had good enzyme and cell potency but showed no improvement in selectivity (**11i−11k**). Additionally, placement of a methoxy substituent at C-2′ produced a significant decrease in enzyme and cell potency (**11l**). When the phenyl ring was replaced with a pyridine ring (**12a**), an increase in enzyme and cell potency was realized, but selectivity still remained low. By installing a methyl group at the C-6′ position of this pyridine ring (**12b**) an increase in selectivity was achieved similar to what was observed for the phenyl analogues (**11a−g**). Although the solubility of **12b** was moderate, its excellent cell activity made it an attractive compound.

Following the procedure established by Kothe,[14] we determined the crystal structure of the PLK1 kinase domain (residues 13−345, T210 V mutant) in complex with **12b** at 2.6 Å resolution. Compound **12b** binds in the hinge region of the kinase domain, forming key hydrogen bonds between the aminopyrimidine and the main chain atoms of Cys-133, as well as an unusual heterocyclic CH−O hydrogen bond with the main chain carbonyl of Glu-131 (Figure 2). Similar hinge-binding interactions have been reported in previous PLK1 crystal structures with inhibitors bound.[15] Also, the 3-dimethylaminopropyl group forms a hydrogen bond with the side chain carboxylate of Glu-140.[16] This key interaction helps to characterize the SAR observed around the upper phenyl ring and the increased activity observed for **10n** over related phenyl analogues (Table 2). Another important interaction involves a hydrogen bond between the thiolactam NH group and the side chain of Asp194 from the DFG motif of this kinase. In addition, the 6′-Me substituent on the pyridine ring fits into a small selectivity pocket near residue Leu-132. This hinge residue was identified previously as a key determinant of PLK1 inhibitor selectivity over related kinases that possess a bulkier residue (Phe or Tyr) at this position.[15] This structural feature of PLK1 helps inform the SAR and selectivity observed by increased steric bulk at C-6′ of the phenyl and pyridine ring described previously (see Table 3).
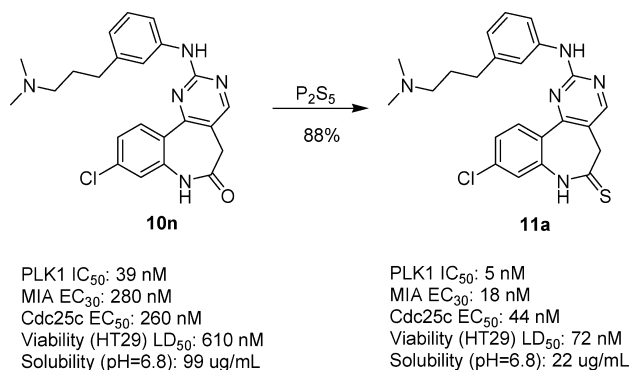
Having discovered a compound (**12b**) with excellent in vitro activities and a promising selectivity profile, we hoped to build upon this discovery and further optimize this series. Previously, we determined that a variety of functional groups were tolerated at the C-9 position of the benzolactam core (see Table 1). After discovery of **12b**, the methylpyridine functionality became the favored appendage off of the amino-pyrimidine for analogue construction. Consequently, we constructed analogues that combined the methylpyridine group with a number of functionalities at C-9. Out of this effort we identified **12c** (MLN0905),[17] a trifluoromethyl replacement of the chloro substituent (Table 4). Like its precursor, **12c** displayed excellent enzyme and cell potency but achieved a significant increase in solubility. Additionally, both of these compounds were screened in an extensive kinase panel (Ambit) to determine a wider selectivity profile. Evaluation of **12b** and **12c** against a panel of 359 kinases revealed them to be reasonably selective inhibitors of PLK1.[18]

Table 2. SAR of Upper Phenyl Ring[b]
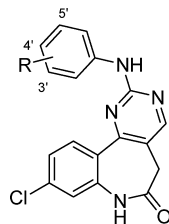
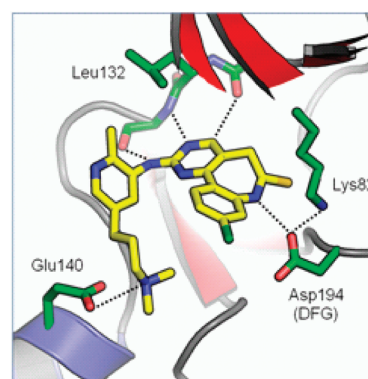|	R	PLK1 IC$_{50}$ (nM)	Solubility (μg/mL)[a]	MIA EC$_{30}$ (μM)	Cdc25c EC$_{50}$ (μM)	Cell viability HT29 LD$_{50}$ (μM)
1	3`-OMe; 4`-OMe	31 ± 10	11	0.88	1.4	3.3 ± .15
10a	3`-OMe	120 ± 14	25	-	-	18
10b	4`-OMe	78 ± 36	3	-	-	2.0
10c	3`-OMe; 5`-OMe	33 ± 3	20	>10	-	-
10d	3`,4`,5`-H	370	4	-	-	-
10e	3`-CO$_2$H	39	-	-	-	>25
10f	4`-CO$_2$H	36 ± 8	81	>10	-	-
10g	4`-I	120 ± 26	3	>10	-	-
10h	4`- (CH$_2$)$_3$NH$_2$	340 ± 138	47	-	-	-
10i	4`- (N-methylpiperazinyl)	260 ± 75	87	>10	-	1.3
10j	4`- C(O)NH$_2$	21	3	-	-	23
10k	4`- C(O)NH-cyclopentyl	12 ± 8	6	0.42	0.63	1.2 ± 0.24
10l	4`- SO$_2$N(Et)$_2$	420 ± 40	6	-	-	3.4
10m	3`- C(O)NHCH$_2$CH$_2$-morpholine	520	-	-	-	12
10n	3`- (CH$_2$)$_3$N(CH$_3$)$_2$	39 ± 12	99	0.28 ± .08	0.26	0.61 ± .20
10o	3`- CH$_2$-(N-methylpiperazinyl)	730	1	-	-	2.9
10p	3`- cyclopropyl-CH$_2$N(CH$_3$)$_2$	130	96	-	-	0.82
10q	3`- OCH$_2$CH$_2$N(CH$_3$)$_2$	130	>99		-	1.2
10r	3`- CH$_2$-morpholine	290	12	-	-	15

[a]pH = 6.8. [b]Standard deviations are reported for $N \geq 3$. Otherwise IC$_{50}$, EC$_{30}$, and LD$_{50}$ values are mean values of two determinations.

Scheme 3. Conversion of Lactam to Thiolactam

10n

PLK1 IC$_{50}$: 39 nM
MIA EC$_{30}$: 280 nM
Cdc25c EC$_{50}$: 260 nM
Viability (HT29) LD$_{50}$: 610 nM
Solubility (pH=6.8): 99 ug/mL

11a

PLK1 IC$_{50}$: 5 nM
MIA EC$_{30}$: 18 nM
Cdc25c EC$_{50}$: 44 nM
Viability (HT29) LD$_{50}$: 72 nM
Solubility (pH=6.8): 22 ug/mL

Figure 2. Crystal structure of PLK1 bound to **12b**. The crystal structure is available from the RCSB PDB with access code 3THB and is further described in the Supporting Information.

We then advanced these compounds into an evaluation of their in vivo properties. While chemical modification of the C-9 position resulted in little effect on the in vitro potency profiles of these compounds, evaluation of the in vivo pharmacokinetic (PK) properties and pharmacodynamic (PD) responses to these inhibitors did allow for differentiation.

PLK1 inhibitors elicit mitotic arrest as a pathway effect.[19] This effect has been confirmed in both cells and xenografts based on the mitotic marker histone H3 (Ser10), as the phosphorylation of histone H3 (pH3) is a readout of PLK1 pathway modulation.[20] By inhibiting PLK1, we expected that cells would be arrested/delayed in mitosis and this could be measured by an increase in pH3. Accordingly, accumulation of pH3 as a pathway biomarker and PD readout of PLK1 inhibition was exploited in these studies.

Compounds **12b** and **12c** were administered as single oral doses (50 mg/kg) to nude mice bearing HT29 xenograft tumors and plasma and tumor compound concentrations were measured at 24, 48, and 72 h post dose. PD effects were analyzed in tumor tissue by immunofluorescent staining to determine the percentage of tumor area staining positive for pH3. Administration of both compounds resulted in sustained (24 h) tumor tissue concentrations of >1 μM (Figure 3). A corresponding robust PD effect (>30%) was also noted at 24 and 48 h for both compounds. These data suggest a trend whereby efficient and sustained distribution of inhibitor to the tumor is important for a significant and prolonged PD response. Overall, **12c** showed a higher sustained PD response as it impressively generated a robust PD response up to 72 h

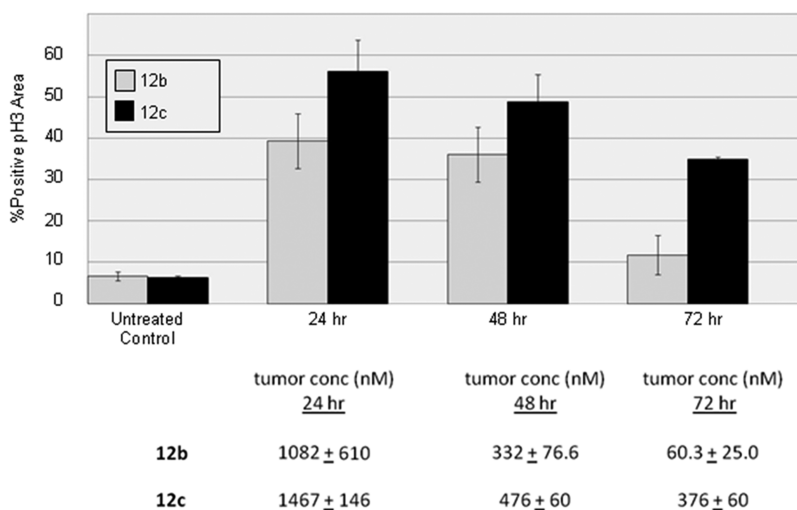## Table 3. SAR of Upper Aryl Ring and Kinase Selectivity[a]

11: X = C
12: X = N
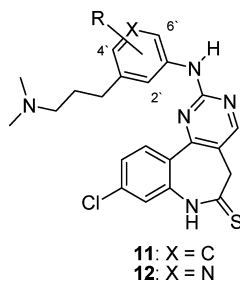
	R	solubility (μg/mL)[b]	PLK1 IC$_{50}$ (nM)	cell activity (nM)			kinase selectivity IC$_{50}$ (nM)					
				MIA EC$_{30}$	HT29 LD$_{50}$	Cdc25c EC$_{50}$	PLK3	KDR	PDGFRb	FLT3	FGFR1	KIT
11a	H	24	5 ± 10	18 ± 5	72 ± 37	44	12	10	19	28	12	63
11b	6'-Me	100	2 ± 0.4	32	44 ± 15	64	18	10	49	720	1600	160
11c	6'-Cl	52	1 ± 0.8	53 ± 14	96 ± 20	440	73	56	93	970	2800	720
11d	6'-OMe	12	10	22	180 ± 48	130	140	54	190	590	1000	1100
11e	6'-OCF$_3$	28	7	48	150		260	190	1100	1600	2000	2600
11f	6'-CF$_3$	28	4	160	250		1500	310	550	5600	4100	2300
11g	6'-i-Pr		8	150	380		1100	1400	1600			
11h	5'-Cl	3	1	37	120	150	5					
11i	4'-F	13	2	17	55	38	7	21	23			
11j	4'-OMe	6	1 ± 0.4	18	26 ± 1	32	5	1	27			
11k	4'-CF$_3$	4	1	59	83		9	51	72			
11l	2'-OMe	51	470		5400							
12a	H	22	1 ± 0.5	11 ± 5	34 ± 9	53	31	11	27	95	11	20
12b	6'-Me	50	2 ± 0.8	9 ± 3	17 ± 7	33 ± 21	64	130	49	730	200	610

[a]Standard deviations are reported for N ≥ 3. Otherwise IC$_{50}$, EC$_{30}$, and LD$_{50}$ values are mean values of two determinations. [b]pH = 6.8.

Table 4. Methylpyridine Analogues[a]

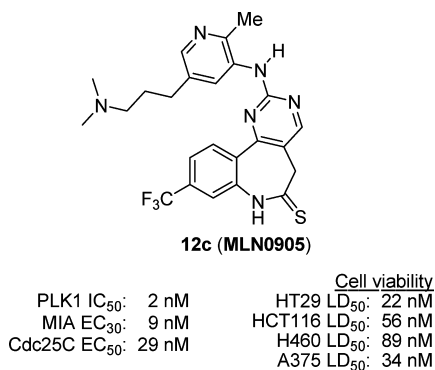|	R	solubility ($\mu g/mL$)[b]	PLK1 IC$_{50}$ (nM)	MIA EC$_{30}$ (nM)	Cdc25C EC$_{50}$ (nM)	cell viability HT29 LD$_{50}$ (nM)	kinase selectivity (359 kinases screened at 1 μM inhibitor)
12b	Cl	50	2 ± 0.8	9 ± 3	33 ± 21	17 ± 7	37 kinases ≥65% inh
							14 kinases ≥90% inh
12c	CF$_3$	105	2 ± 0.8	9 ± 3	29 ± 20	22 ± 10	28 kinases ≥65% inh
							10 kinases ≥90% inh

[a]Standard deviations are reported for $N \geq 3$. Otherwise IC$_{50}$, EC$_{30}$, and LD$_{50}$ values are mean values of two determinations. [b]pH = 6.8.

	tumor conc (nM) 24 hr	tumor conc (nM) 48 hr	tumor conc (nM) 72 hr
12b	1082 ± 610	332 ± 76.6	60.3 ± 25.0
12c	1467 ± 146	476 ± 60	376 ± 60

Figure 3. Comparison of PD response of **12b** and **12c** following a single 50 mg/kg po dose (vehicle: 10% HPβCD/2.5% dextrose in water).

after a single 50 mg/kg dose. In contrast, pH3 levels for **12c** had returned back to near baseline levels at this time point.

12c also proved itself to be a potent inhibitor of PLK1 in cells (Figure 4) in addition to being a reasonably selective

12c (MLN0905)

	Cell viability	
PLK1 IC$_{50}$: 2 nM	HT29 LD$_{50}$: 22 nM	
MIA EC$_{30}$: 9 nM	HCT116 LD$_{50}$: 56 nM	
Cdc25C EC$_{50}$: 29 nM	H460 LD$_{50}$: 89 nM	
	A375 LD$_{50}$: 34 nM	

Figure 4. In vitro activity profile of **12c**.

inhibitor of PLK1 (Table 4). From the kinase selectivity screen, none of the inhibited kinases would be expected to contribute to the cellular and PD effects observed.[18] Moreover, the cellular phenotype observed with **12c** treatment, G2-M arrest and

monopolar spindle formation, is consistent with that of PLK1 RNAi treatment and small molecule PLK1 inhibition (data not shown).[20b,21] Combined with its excellent in vitro potency, good solubility, and ability to generate a prolonged PD response in vivo, **12c** differentiated itself sufficiently to become our lead compound and warrant further investigation into its in vivo properties.

The PK properties of **12c** were further characterized in female nude NCR mice bearing HT29 tumors and naïve male Sprague−Dawley (SD) rats after intravenous (IV) and oral dosing (Table 5). In general, the PK of **12c** was characterized by moderate to high systemic clearance (CL$_P$), high volume of distribution (V_{SS}), moderate apparent elimination half-life ($t_{1/2}$), and moderate bioavailability (%F) in both species. The plasma protein binding of **12c** was moderate to high (87.4−94.3%) and concentration-independent in the range of 0.5−5 μM in mice and rats. In nude NCR mice bearing HT29 xenografts, **12c** is rapidly and extensively distributed to tumor with a tumor-to-plasma AUC$_{0-24h}$ ratio of 10.4 after a single PO dose of 12.5 mg/kg.

Encouraged by the initial PD response observed with **12c** (50 mg/kg dose in Figure 3) and its efficient distribution to tumor tissue, additional PD studies were conducted in nude mice bearing HT29 xenograft tumors. Following single oral

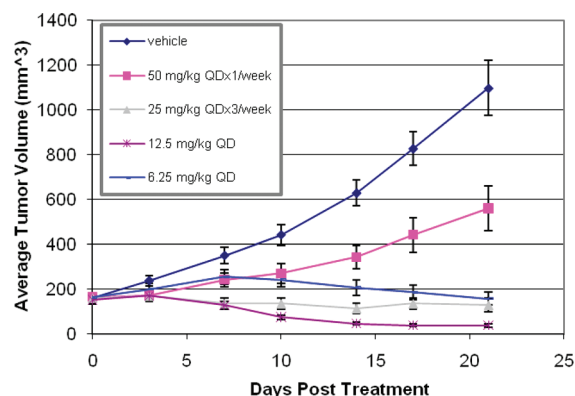**Table 5. Summary of 12c Pharmacokinetic Properties**

species	CL_P $(L/h/kg)^a$	V_{SS} $(L/kg)^a$	$t_{1/2}$ $(h)^a$	C_{max} $(nM)^b$	T_{max} $(h)^b$	F $(\%)^c$
rat, SD	2.3	10.2	4.7	335	4.0	72
mouse, NCR nude	2.5	6.2	3.4	720	4.0	45

$^a CL_P$, V_{SS}, and $t_{1/2}$ are from IV studies (dosed at 2 mg/kg in mice, 1 mg/kg in rats). $^b C_{max}$ and T_{max} are from PO studies (dosed at 12.5 mg/kg in mice, 5 mg/kg in rats). $^c F$ (%) was calculated relative to the listed respective IV doses versus PO dose (12.5 mg/kg in mice, 5 mg/kg in rats). Vehicle: 10% HPβCD/2.5% dextrose in water.

Figure 6. Tumor growth Inhibition following oral administration of **12c** in mice bearing HT29 xenograft tumors (vehicle: 10% HPβCD/2.5% dextrose in water).

doses of 25, 12.5, and 6.25 mg/kg, a PD dose response was observed (Figure 5). A robust PD effect was sustained for the 25 and 12.5 mg/kg dosing groups for 48 h after administration of **12c**, and a lesser PD response was observed in the 6.25 mg/kg group. Comparison with the 50 mg/kg dosing group discussed previously (data from Figure 3) demonstrated a proportional dose response across all the dosing groups. Accordingly, the concentration of **12c** observed in tumor samples was also proportional across the dosing groups (Figure 5). These data indicate a concentration dependent PD response whereby greater tumor exposure of **12c** yields a greater PD response.
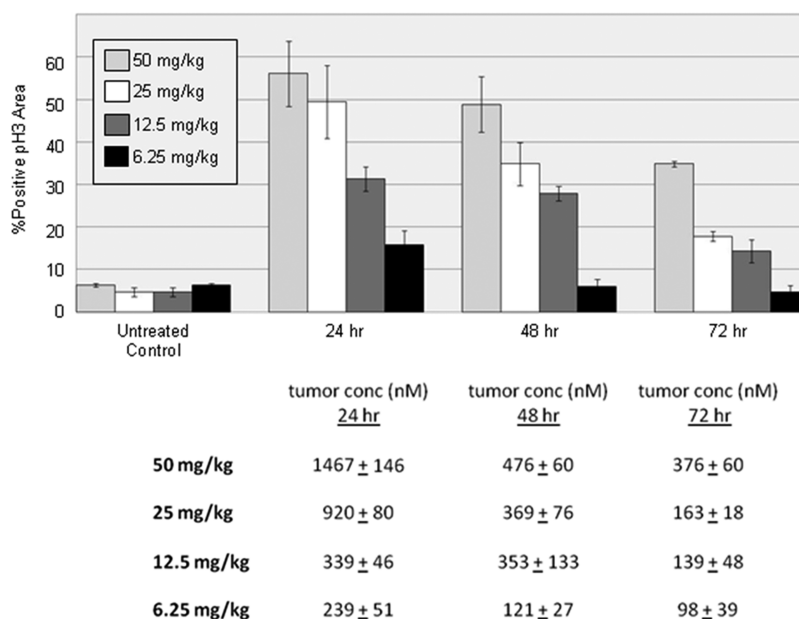
Ensuing tolerability studies were initiated in nude mice to determine the maximum tolerated dose (MTD) for **12c** dosed on a variety of different schedules. Results from these experiments determined the following MTDs: daily (QD), 12.5 mg/kg; QD×1/week, 50 mg/kg; and QD×3/week, 25 mg/kg (data not shown).

Having established MTDs for **12c**, the antitumor effect of **12c** was next evaluated in nude mice bearing HT29 xenograft tumors. Mice (10 animals/group) were treated orally with **12c** for 21 days at doses based on tolerability results: QD (6.25 and 12.5 mg/kg), QD×1/week (50 mg/kg), and QD×3/week (25 mg/kg) (Figure 6). Significant antitumor activity ($p < 0.005$) was observed using all doses and schedules in this study, and all doses and schedules were tolerated throughout the

course of the study with mean body weight loss less than 10%. While 50 mg/kg dosed once/week achieved tumor growth inhibition (T/C = 0.53, $p < 0.005$), tumor stasis and regression were achieved with more continuous exposure to drug, even at low doses. By altering the administration schedule of **12c** to 3 days on/4 days off (QD×3/week, 25 mg/kg), a significant decrease in T/C was observed (0.14, $p < 0.0001$). Following a schedule of daily administration of 6.25 mg/kg, a significant inhibition of tumor growth was also accomplished (T/C = 0.15, $p < 0.0001$). Ultimately, tumor regressions were observed through daily treatment with 12.5 mg/kg of **12c** (T/C = 0.03, $p < 0.0001$). In the 12.5 mg/kg group, the mean body weight loss for the group was <5%, however one animal was removed from the study between days 10−14 due to body weight loss of >16%. In the 12.5 mg/kg QD group, three of the nine mice which completed the 21 day treatment phase had no measurable tumor (i.e., complete response) out to 70 days post treatment initiation.

	tumor conc (nM) 24 hr	tumor conc (nM) 48 hr	tumor conc (nM) 72 hr
50 mg/kg	1467 ± 146	476 ± 60	376 ± 60
25 mg/kg	920 ± 80	369 ± 76	163 ± 18
12.5 mg/kg	339 ± 46	353 ± 133	139 ± 48
6.25 mg/kg	239 ± 51	121 ± 27	98 ± 39

Figure 5. Dose dependent pH3 PD modulation in HT29 xenograft tumors following a single oral dose of **12c** in nude mice (vehicle: 10% HPβCD/2.5% dextrose in water).

CONCLUSION

In conclusion, a series of small molecule inhibitors of PLK1 was identified and described in this report. Optimization of an HTS hit (**1**) led to the discovery of **12c**, a potent inhibitor of PLK1 in cells confirmed by inhibition of Cdc25C-T96 phosphorylation, a direct cellular readout of PLK1 inhibition. **12c** also demonstrated the ability to impede cell proliferation in numerous human tumor cell lines. Growth inhibition in these cell lines was consistent with mitotic arrest or delay, which are known to be a result of PLK1 inhibition. This effect was confirmed by in vivo PD experiments that showed increased levels of phosphorylation of the mitotic pathway marker histone H3 (Ser10) in xenografts after exposure to **12c**. In vivo antitumor activity of **12c** was observed in the HT29 colon xenograft model, with tumor stasis or regression observed at oral doses that were well-tolerated. Additionally, there was flexibility in the administration of **12c** because various treatment schedules (intermittent and continuous) demonstrated antitumor activity in this model. Taken together these data demonstrate that **12c** is a pharmacologically active compound whose effects are consistent with PLK1 inhibition.

EXPERIMENTAL SECTION

NMR spectra were recorded in the solvent reported on a Bruker 300 MHz Avance 1 or 400 MHz Avance 2 (5 mm QnProbe) using residual solvent peaks as the reference. Compound purity was determined by analysis of the diode array UV trace of an LC-MS spectrum using the following procedure: compounds were dissolved in DMSO, methanol, or acetonitrile, and the solutions were analyzed using an Agilent 1100 LC interfaced to a micromass Waters Micromass Zspray mass detector (ZMD). One of two gradients was used to elute the compounds; either a formic acid (FA) gradient (acetonitrile containing 0−100% 0.1% formic acid in water) or an ammonium acetate (AA) gradient (acetonitrile containing zero to 100% 10 mM ammonium acetate in water). All compounds were determined to be >95% pure unless otherwise noted.

9-Chloro-2-(3,4-dimethoxyphenylamino)-5H-benzo[b]-pyrimido[4,5-d]azepin-6(7H)-one (1). *General Procedure A.* Step 1: To a 250 mL round-bottom flask with magnetic stirrer was added 8-chloro-3,4-dihydro-1H-1-benzazepine-2,5-dione (**3**; R = Cl) (52.0 g, 0.248 mol) and THF (364 mL). 1,1-Dimethoxy-N,N-dimethylmethanamine (175 mL, 1.24 mol) was added, and then the flask was fitted with a reflux condenser. The resulting reaction mixture was heated at 60 °C under an atmosphere of argon for 2 h. The light-orange solution with a suspended solid was allowed to cool to room temperature. Ether (250 mL) was added, and the precipitated material was collected via suction filtration, washed with ether, and dried in vacuum oven (40 °C) for 2 days to give 62 g (94%) of **4** (R = Cl) as a gray solid. ^{1}H NMR (400 MHz, DMSO) δ 10.05 (s, 1H), 7.72 (d, *J* = 8.5 Hz, 1H), 7.62 (s, 1H), 7.23−7.16 (m, 1H), 7.08 (d, *J* = 2.1 Hz, 1H), 3.33 (s, 2H), 3.23 (s, 6H). LCMS (FA) *m/z* = 265.2 (M + H).

Step 2: A mixture of **4** (R = Cl) (101 mg, 0.382 mmol), N-(3,4-dimethoxyphenyl)guanidine·HNO₃ (118 mg, 0.458 mmol), and potassium carbonate (132 mg, 0.954 mol) in ethanol (2.7 mL) was heated to reflux overnight. The mixture was cooled to room temperature and added to water (20 mL). The resulting suspension was stirred for 2 h, and the solid was collected by filtration and dried to give 136 mg (90%) of **1**. ^{1}H NMR (400 MHz, DMSO) δ 10.35 (s, 1H), 9.60 (s, 1H), 8.49 (s, 1H), 8.11 (d, *J* = 8.5 Hz, 1H), 7.69 (s, 1H), 7.41 (dd, *J* = 8.5, 2.1 Hz, 1H), 7.28 (d, *J* = 2.1 Hz, 1H), 7.22 (dd, *J* = 8.7, 2.4 Hz, 1H), 6.89 (d, *J* = 8.8 Hz, 1H), 3.75 (s, 3H), 3.72 (s, 3H), 3.39 (s, 2H). LCMS (FA) *m/z* = 397.1 (M + H).

9-Iodo-2-(3,4-dimethoxyphenylamino)-5H-benzo[b]-pyrimido[4,5-d]azepin-6(7H)-one (5a). Prepared by general procedure A using **3** (R = I) in step 1.
^{1}H NMR (300 MHz, DMSO) δ 10.24 (s, 1H), 9.57 (s, 1H), 8.46 (s, 1H), 7.83 (d, *J* = 8.3 Hz, 1H), 7.74−7.62 (m, 2H), 7.59 (s, 1H), 7.22 (dd, *J* = 8.7, 2.3 Hz, 1H), 6.88 (d, *J* = 8.8 Hz, 1H), 3.74 (s, 3H), 3.70 (s, 3H), 3.36 (s, 2H). LCMS (FA) *m/z* = 489 (M + H).

9-Trifluoromethyl-2-(3,4-dimethoxyphenylamino)-5H-benzo[b]pyrimido[4,5-d]azepin-6(7H)-one (5b). Prepared by general procedure A using **3** (R = CF₃) in step 1.
^{1}H NMR (300 MHz, DMSO) δ 10.44 (s, 1H), 9.63 (s, 1H), 8.51 (s, 1H), 8.27 (d, *J* = 8.1 Hz, 1H), 7.66 (d, *J* = 8.6 Hz, 2H), 7.54 (s, 1H), 7.22 (dd, *J* = 8.8, 2.4 Hz, 1H), 6.87 (d, *J* = 8.8 Hz, 1H), 3.73 (s, 3H), 3.69 (s, 3H), 3.41 (s, 2H). LCMS (FA) *m/z* = 431 (M + H).

2-(3,4-Dimethoxyphenylamino)-5H-benzo[b]pyrimido[4,5-d]azepin-6(7H)-one (5c). Prepared by general procedure A using **3** (R = H) in step 1.
^{1}H NMR (400 MHz, DMSO) δ 10.22 (s, 1H), 9.53 (s, 1H), 8.47 (s, 1H), 8.10 (dd, *J* = 7.9, 1.4 Hz, 1H), 7.72 (s, 1H), 7.63−7.50 (m, 1H), 7.38−7.28 (m, 1H), 7.28−7.18 (m, 2H), 6.89 (d, *J* = 8.8 Hz, 1H), 3.76 (s, 3H), 3.72 (s, 3H), 3.35 (s, 2H). LCMS (FA) *m/z* = 363.2 (M + H).

9-Fluoro-2-(3,4-dimethoxyphenylamino)-5H-benzo[b]-pyrimido[4,5-d]azepin-6(7H)-one (5d). Prepared by general procedure A using **3** (R = F) in step 1.
^{1}H NMR (300 MHz, DMSO) δ 10.34 (s, 1H), 9.56 (s, 1H), 8.46 (s, 1H), 8.14 (dd, *J* = 8.8, 6.7 Hz, 1H), 7.68 (s, 1H), 7.21 (ddd, *J* = 10.8, 5.3, 2.5 Hz, 2H), 7.02 (dd, *J* = 10.4, 2.5 Hz, 1H), 6.88 (d, *J* = 8.8 Hz, 1H), 3.74 (s, 3H), 3.71 (s, 3H), 3.38 (s, 2H). LCMS (FA) *m/z* = 381.1 (M + H).

9-Methyl-2-(3,4-dimethoxyphenylamino)-5H-benzo[b]-pyrimido[4,5-d]azepin-6(7H)-one (5e). Prepared by general procedure A using **3** (R = Me) in step 1.
^{1}H NMR (300 MHz, DMSO) δ 10.16 (s, 1H), 9.52 (s, 1H), 8.44 (s, 1H), 7.99 (d, *J* = 8.0 Hz, 1H), 7.72 (s, 1H), 7.18 (dd, *J* = 23.7, 8.4 Hz, 2H), 7.01 (s, 1H), 6.88 (d, *J* = 8.8 Hz, 1H), 3.75 (s, 3H), 3.71 (s, 3H), 3.33 (s, 2H), 2.36 (s, 3H). LCMS (FA): *m/z* = 377.4 (M + H).

9-Cyano-2-(3,4-dimethoxyphenylamino)-5H-benzo[b]-pyrimido[4,5-d]azepin-6(7H)-one (5f). A mixture of **5a** (100 mg, 0.21 mmol), Zn(CN)₂ (14 mg, 0.12 mmol), Pd₂(dba)₃ (9.5 mg, 0.01 mmol), and dppf (14 mg, 0.02 mmol) was stirred in DMF (2 mL). A drop of water was added and the mixture heated at 120 °C overnight with stirring. The reaction was then allowed to cool to room temperature and diluted with EtOAc and a solution of saturated NaHCO₃ (aq). The organic layer was separated and washed with brine and water, then dried over MgSO₄, filtered, and concentrated. The crude product was purified on silica gel to give **5f** (75 mg, 92%). ^{1}H NMR (300 MHz, DMSO) δ 10.46 (s, 1H), 9.65 (s, 1H), 8.53 (s, 1H), 8.24 (d, *J* = 8.2 Hz, 1H), 7.76 (dd, *J* = 8.2, 1.6 Hz, 1H), 7.66 (s, 1H), 7.61 (d, *J* = 1.4 Hz, 1H), 7.20 (dd, *J* = 8.7, 2.4 Hz, 1H), 6.88 (d, *J* = 8.8 Hz, 1H), 3.74 (s, 3H), 3.70 (s, 3H), 3.41 (s, 2H). LCMS (FA) *m/z* = 388.2 (M + H).

2-Amino-9-chloro-5H-benzo[b]pyrimido[4,5-d]azepin-6(7H)-one (8). To a solution of **4** (R = Cl) (11.8 g, 44.6 mmol) in EtOH (300 mL) was added guanidine hydrochloride (4.68 g, 49.0 mmol) and potassium carbonate (20.0 g, 145 mmol). The reaction mixture was allowed to stir, overnight, at 75 °C. Most of the solvent was removed in vacuo, and the remaining mixture was diluted in water (500 mL). The resulting solution was stirred, at room temperature, for 30 min. The cloudy mixture was filtered and washed with water and MeOH to give **8** (10.5 g, 90%) as a white solid. ^{1}H NMR (400 MHz, DMSO) δ 10.24 (s, 1H), 8.25 (s, 1H), 7.99−7.89 (m, 1H), 7.33 (dd, *J* = 8.5, 2.1 Hz, 1H), 7.22 (d, *J* = 2.1 Hz, 1H), 6.74 (s, 2H), 3.27 (s, 2H). LCMS (FA): *m/z* = 261.1 (M + H)

9-Chloro-2-(phenylamino)-5H-benzo[b]pyrimido[4,5-d]-azepin-6(7H)-one (10d). To a solution of **8** (148 mg, 0.568 mmol), 1-bromobenzene (0.072 mL, 0.681 mmol), Cs₂CO₃ (333 mg, 1.02 mmol), and BINAP (53 mg, 0.085 mmol) in 4 mL of toluene was added Pd(OAc)₂ (12.8 mg, 0.057 mmol), and the reaction was stirred at 100 °C for 12 h. The reaction mixture was then treated with H₂O and extracted with CH₂Cl₂ (2 × 30 mL). The organic fractions were combined, filtered, dried over MgSO₄, and concentrated in vacuo to give an orange oil, which was purified by HPLC to afford **10d** (1.8 mg, 0.9%). ^{1}H NMR (300 MHz, DMSO) δ 10.35 (s, 1H), 9.77 (s, 1H), 8.53 (s, 1H), 8.08 (d, *J* = 8.6 Hz, 1H), 7.80 (d, *J* = 7.9 Hz, 2H), 7.43 (dd, *J* = 8.5, 2.0 Hz, 1H), 7.29 (m, 3H), 6.95 (t, *J* = 7.2 Hz, 1H), 3.41

(s, 2H). HRMS calcd for $C_{18}H_{13}ClN_4O$, 337.0856; found, 337.0853 (M + H).

2-(3-(3-Aminopropyl)phenylamino)-9-chloro-5H-benzo[b]-pyrimido[4,5-d]azepin-6(7H)-one (10n). To a microwave tube was added 3-(3-bromophenyl)-N,N-dimethylpropan-1-amine (1.53 g, 6.31 mmol), **8** (1.64 g, 6.31 mmol), cesium carbonate (2.88 g, 8.83 mmol), 4,5-bis(diphenylphosphino)-9,9-dimethylxanthene (0.22 g, 0.38 mmol), and tris(dibenzylideneacetone)dipalladium (0) (0.23 g, 0.25 mmol) and dioxane (30 mL). The resulting mixture was heated at 150 °C for 70 min in a microwave reactor. The reaction mixture was cooled to room temp, then 80 mL of THF was added to the mixture. It was then filtered, and the filtrate was concentrated. The crude residue was purified on silica gel to give **10n** (1.92 g; 72%). ^{1}H NMR (400 MHz, DMSO) δ 10.35 (s, 1H), 9.69 (s, 1H), 8.51 (s, 1H), 8.08 (d, J = 8.5 Hz, 1H), 7.73 (s, 1H), 7.60−7.50 (m, 1H), 7.40 (dd, J = 8.5, 2.1 Hz, 1H), 7.27 (d, J = 2.1 Hz, 1H), 7.17 (t, J = 7.8 Hz, 1H), 6.78 (d, J = 7.6 Hz, 1H), 3.39 (s, 2H), 2.60−2.51 (m, 2H), 2.20 (t, J = 7.2 Hz, 2H), 2.10 (s, 6H), 1.69 (dt, J = 14.7, 7.5 Hz, 2H). LCMS (FA): m/z 422.0 (M + H).

9-Chloro-2-({3-[3-(dimethylamino)propyl]phenyl}amino)-5,7-dihydro-6H-pyrimido[5,4-d][1]benzazepine-6-thione (11a). *General Procedure B.* Thioamide formation using phosphorus pentasulfide.

A mixture of **10s** (940 mg, 2.2 mmol) and phosporous pentasulfide (1.14 g, 5.12 mmol) in pyridine (17 mL) was allowed to stir overnight at 60 °C. At this point, additional phosporous pentasulfide (66 mg, 0.30 mmol) was added and the reaction mixture was allowed to stir for another 1 h. The reaction mixture was then added dropwise into a stirred soln of 1:1 water/1 M aq NaHCO$_3$ solution (160 mL) and allowed to stir for an hour. The resulting solid was obtained after filtration and a wash with water and ether. The yellowish−tan solid obtained was vacuum-dried to give **11a** (980 mg; 100%). LCMS (FA): m/z 438.2 (M + H).

11a (920 mg, 2.1 mmol) was then dissolved in tetrahydrofuran (37 mL), and to this 2.00 M of HCl in ether (2.10 mL, 4.20 mmol) was added and allowed to stir for 10 min. Ether (170 mL) was added and then allowed to stir for 30 min. The resulting solid was filtered and washed with ether and dried under vacuum to give **11a** as the bis-HCl salt (944 mg; 88%). ^{1}H NMR (400 MHz, DMSO) δ 12.27 (s, 1H), 10.22 (s, 1H), 9.82 (s, 1H), 8.49 (s, 1H), 8.09 (d, J = 8.5 Hz, 1H), 7.67 (s, 1H), 7.62 (d, J = 8.1 Hz, 1H), 7.56 (dd, J = 8.5, 1.9 Hz, 1H), 7.42 (d, J = 1.8 Hz, 1H), 7.22 (t, J = 7.8 Hz, 1H), 6.84 (d, J = 7.4 Hz, 1H), 3.85 (s, 2H), 3.03 (m, 2H), 2.72 (s,3H), 2.71(s, 3H), 2.60 (m, 2H), 1.95 (m, 2H). LCMS (FA): m/z 438.2 (M + H).

9-Chloro-2-(5-(3-(dimethylamino)propyl)-2-methylphenyla-mino)-5H-benzo[b]pyrimido[4,5-d]azepine-6(7H)-thione (11b). General procedure B using P$_2$S$_5$ was used to give **11b** as the formate salt after HPLC purification (115 mg, 29%). ^{1}H NMR (300 MHz, DMSO) δ 8.94 (s, 1H), 8.37 (s, 1H), 7.94 (m, 1H), 7.46 (dd, J = 8.5, 1.9 Hz, 1H), 7.41−7.33 (m, 2H), 7.11 (d, J = 7.7 Hz, 1H), 6.89 (d, J = 7.5 Hz, 1H), 3.80 (s, 2H), 3.74 (d, J = 5.3 Hz, 1H), 2.59−2.51 (m, 2H), 2.45−2.34 (m, 2H), 2.23 (s, 6H), 2.18 (s, 3H), 1.81−1.64 (m, 2H). LC-MS (FA): m/z 452.2 (M + H).

9-Chloro-2-({2-chloro-5-[3-(dimethylamino)propyl]phenyl}-amino)-5,7-dihydro-6H-pyrimido[5,4-d][1]benzazepine-6-thi-one (11c). General procedure B using P$_2$S$_5$ was used to give **11c** as the formate salt after HPLC purification (1.9 g, 46%). ^{1}H NMR (400 MHz, DMSO) δ 9.03 (s, 1H), 8.46 (s, 1H), 8.23 (s, 1H), 7.99 (d, J = 8.5 Hz, 1H), 7.68 (d, J = 1.6 Hz, 1H), 7.49 (dd, J = 8.5, 2.0 Hz, 1H), 7.41 (s, 1H), 7.40 (d, J = 5.1 Hz, 1H), 7.02 (dd, J = 8.2, 1.8 Hz, 1H), 3.86 (s, 2H), 2.59 (m, 2H), 2.36 (m, 2H), 2.22 (s, 6H), 1.81−1.68 (m, 2H). LCMS (FA): m/z 472.1 (M + H).

9-Chloro-2-({5-[3-(dimethylamino)propyl]-2-methoxyphenyl}amino)-5,7-dihydro-6H-pyrimido[5,4-d][1]-benzazepine-6-thione (11d). *General Procedure C.* Thioamide formation using Lawesson's reagent.

Into a round-bottomed flask was added **SI-25** (0.18 g, 0.40 mmol), 2,4-bis(4-methoxyphenyl)-2,4-dithioxo-1,3,2,4-dithiadiphosphetane (0.33 g, 0.81 mmol), and THF (6 mL). The mixture was stirred at 60 °C for 1 h. The mixture was then partitioned between DCM (50 mL) and satd NaHCO$_3$ (aq) (20 mL). The organic phase was washed with water and brine. The solution was then dried over Na$_2$SO$_4$, filtered, and concentrated. The residue was triturated with ether to give a yellow solid, which was redissolved in THF. 2N HCl in ether was added to give a yellow solid which was collected by filtration. Obtained **11d** as the HCl salt (160 mg, 85%). ^{1}H NMR (400 MHz, MeOD) δ 8.04 (s, 1H), 7.81 (d, J = 8.5 Hz, 1H), 7.48 (s, 1H), 7.15 (dd, J = 8.5, 2.0 Hz, 1H), 7.04 (d, J = 2.0 Hz, 1H), 6.80 (d, J = 8.3 Hz, 1H), 6.70 (d, J = 8.4 Hz, 1H), 3.68 (s, 2H), 3.60 (s, 3H), 2.79 (m, 2H), 2.53 (s, 6H), 2.43 (m, 2H), 1.80 (m, 2H). LCMS (FA): m/z 468.9 (M + H).

9-Chloro-2-{[5-[3-(dimethylamino)propyl]-2-(trifluoromethoxy)phenyl]amino}-5,7-dihydro-6H-pyrimido-[5,4-d][1]benzazepine-6-thione (11e). General procedure C using Lawesson's reagent was used to give **11e** as the formate salt after HPLC purification (60 mg, 32%). ^{1}H NMR (300 MHz, DMSO) δ 9.27 (s, 1H), 8.46 (s, 1H), 8.16 (s, 1H), 7.99 (d, J = 8.5 Hz, 1H), 7.78 (s,1H), 7.49 (d, J = 8.5, 1H), 7.40 (S, 1H), 7.28 (d, J = 8.4, 1H), 7.05 (d, J = 8.41H), 3.85 (s, 2H), 3.76−3.67 (m, 1H), 2.65−2.54 (m, 2H), 2.27 (s, 6H), 1.75 (m, 2H). LCMS (FA): m/z 522.1 (M + H).

9-Chloro-2-(5-(3-(dimethylamino)propyl)-2-(trifluoromethyl)phenylamino)-5H-benzo[b]pyrimido[4,5-d]-azepine-6(7H)-thione (11f). General procedure C using Lawesson's reagent was used to give **11f** as the formate salt after HPLC purification (8 mg, 20%). ^{1}H NMR (300 MHz, DMSO) δ 8.97 (s, 1H), 8.38 (s, 1H), 8.17 (s, 1H), 7.90 (d, J = 8.5 Hz, 1H), 7.63 (d, J = 8.0 Hz, 1H), 7.56 (s, 1H), 7.45 (d, J = 8.5 Hz, 1H), 7.38 (s, 1H), 7.24 (d, J = 7.6 Hz, 1H), 3.82 (s, 2H), 2.65 (m, 2H), 2.31 (m, 2H), 2.18 (s, 6H), 1.74 (m, 2H). LCMS (FA): m/z 506.1 (M + H).

9-Chloro-2-({5-[3-(dimethylamino)propyl]-2-isopropylphenyl}amino)-5,7-dihydro-6H-pyrimido[5,4-d][1]-benzazepine-6-thione (11g). General procedure C using Lawesson's reagent was used to give **11g** as the formate salt after HPLC purification (22 mg, 44%). ^{1}H NMR (400 MHz, DMSO) δ 9.00 (s, 1H), 8.34 (d, J = 9.3 Hz, 1H), 7.93 (d, J = 8.5 Hz, 1H), 7.47 (dd, J = 8.5, 2.0 Hz, 1H), 7.39 (d, J = 2.0 Hz, 1H), 7.23 (d, J = 8.0 Hz, 1H), 7.19 (s, 1H), 7.03 (d, J = 7.8 Hz, 1H), 3.78 (s, 2H), 3.76−3.69 (m, 1H), 3.28 (m, 1H), 3.19 (m, 1H), 2.54 (m, 2H), 2.33 (s, 6H), 1.82−1.69 (m, 2H), 1.11 (d, J = 6.8 Hz, 6H). LCMS (FA): m/z 480.4 (M + H).

9-Chloro-2-({3-chloro-5-[3-(dimethylamino)propyl]phenyl}-amino)-5,7-dihydro-6H-pyrimido[5,4-d][1]benzazepine-6-thi-one (11h). General procedure C using Lawesson's reagent was used to give **11h** as the formate salt after HPLC purification (0.16 g, 41%). ^{1}H NMR (400 MHz, DMSO) δ 10.01 (s, 1H), 8.55 (s, 1H), 8.25 (s, 1H), 8.09 (t, J = 6.7 Hz, 1H), 7.79 (s, 1H), 7.63 (s, 1H), 7.54 (dd, J = 8.5, 2.0 Hz, 1H), 7.43 (d, J = 2.0 Hz, 1H), 6.87 (s, 1H), 3.88 (s, 2H), 2.60−2.54 (m, 2H), 2.45 (s, 2H), 2.29 (s, 6H), 1.76 (s, 2H). LCMS (FA): m/z 472.1 (M + H).

9-Chloro-2-({3-[3-(dimethylamino)propyl]-4-fluorophenyl}-amino)-5,7-dihydro-6H-pyrimido[5,4-d][1]benzazepine-6-thi-one (11i). General procedure B using P$_2$S$_5$ was used to give **11i** as the formate salt after HPLC purification (80 mg, 40%). ^{1}H NMR (300 MHz, DMSO) δ 9.79 (s, 1H), 8.48 (s, 1H), 8.18 (s, 1H), 8.08 (d, J = 8.5 Hz, 1H), 7.76 (d, J = 4.6 Hz, 1H), 7.55 (m, 1H), 7.53−7.48 (m, 1H), 7.41 (d, J = 1.9 Hz, 1H), 7.06 (t, J = 9.3 Hz, 1H), 3.85 (s, 2H), 2.63−2.54 (m, 2H), 2.34 (t, J = 7.1 Hz, 2H), 2.18 (s, 6H), 1.80−1.61 (m, 2H). LCMS (FA): m/z 456.3 (M + H).

9-Chloro-2-({3-[3-(dimethylamino)propyl]-4-methoxyphenyl}amino)-5,7-dihydro-6H-pyrimido[5,4-d][1]-benzazepine-6-thione (11j). General procedure B using P$_2$S$_5$ was used to give **11j** as the formate salt after HPLC purification (54 mg, 29%). ^{1}H NMR (400 MHz, DMSO) δ 9.57 (s, 1H), 8.43 (s, 1H), 8.08 (d, J = 8.5 Hz, 1H), 7.56 (s, 1H), 7.55−7.47 (m, 2H), 7.41 (d, J = 2.1 Hz, 1H), 6.88 (d, J = 8.9 Hz, 1H), 3.82 (s, 2H), 3.74 (s, 3H), 2.56−2.51 (m, 4H), 2.39−2.28 (m, 2H), 2.20 (s, 6H), 1.67 (dt, J = 14.9, 7.6 Hz, 2H). LCMS (FA): m/z 468.4 (M + H).

9-Chloro-2-{3-[3-(dimethylamino)propyl]-4-(trifluoromethyl)phenyl]amino}-5,7-dihydro-6H-pyrimido[5,4-d][1]benzazepine-6-thione (11k). General procedure B using P$_2$S$_5$ was used to give **11k** as the formate salt after HPLC purification (67 mg, 49%). ^{1}H NMR (400 MHz, DMSO) δ 10.22 (s, 1H), 8.59 (s, 1H),

8.18 (s, 1H), 8.14 (d, J = 8.5 Hz, 1H), 8.02 (s, 1H), 7.78 (d, J = 8.8 Hz, 1H), 7.63−7.50 (m, 2H), 7.44 (d, J = 2.1 Hz, 1H), 3.91 (s, 2H), 2.80−2.63 (m, 2H), 2.48−2.41 (m, 2H), 2.26 (s, 6H), 1.77 (m, 2H). LCMS (FA): m/z 506.1 (M + H).

9-Chloro-2-({3-[3-(dimethylamino)propyl]-2-methoxyphenyl}amino)-5,7-dihydro-6H-pyrimido[5,4-d][1]-benzazepine-6-thione (11l). General procedure B using P_2S_5 was used to give **11l** as the formate salt after HPLC purification (10 mg, 49%). ^{1}H NMR (400 MHz, DMSO) δ 8.58 (s, 1H), 8.47 (d, J = 5.5 Hz, 1H), 8.22 (s, 1H), 8.04 (d, J = 8.5 Hz, 1H), 7.84 (dd, J = 8.0, 1.5 Hz, 1H), 7.50 (dd, J = 8.5, 2.1 Hz, 1H), 7.40 (d, J = 2.1 Hz, 1H), 7.04 (t, J = 7.8 Hz, 1H), 6.95 (dd, J = 7.6, 1.5 Hz, 1H), 3.85 (s, 2H), 3.67 (s, 3H), 2.66−2.55 (m, 2H), 2.40−2.31 (m, 2H), 2.21 (s, 6H), 1.72 (m, 2H). LCMS (FA): m/z 468.0 (M + H).

9-Chloro-2-({5-[3-(dimethylamino)propyl]pyridin-3-yl}-amino)-5,7-dihydro-6H-pyrimido[5,4-d][1]benzazepine-6-thi-one (12a). General procedure B using P_2S_5 was used to give **12a** as the formate salt after HPLC purification (46 mg, 20%). ^{1}H NMR (400 MHz, DMSO) δ 9.99 (s, 1H), 8.73 (d, J = 2.3 Hz, 1H), 8.54 (s, 1H), 8.18 (s, 1H), 8.14 (s, 1H), 8.09 (d, J = 8.5 Hz, 1H), 8.03 (d, J = 1.6 Hz, 1H), 7.53 (dd, J = 8.5, 2.0 Hz, 1H), 7.42 (d, J = 2.0 Hz, 1H), 3.88 (s, 2H), 2.57 (dd, J = 18.2, 10.7 Hz, 2H), 2.28 (t, J = 7.2 Hz, 2H), 2.15 (s, 6H), 1.78−1.64 (m, 2H). LCMS (FA): m/z 423.2 (M + H).

9-Chloro-2-({5-[3-(dimethylamino)propyl]-2-methylpyridin-3-yl}amino)-5,7-dihydro-6H-pyrimido[5,4-d][1]benzazepine-6-thione (12b). General procedure B using P_2S_5 was used to give **12b** as the formate salt after HPLC purification (240 mg, 53%). ^{1}H NMR (400 MHz, DMSO) δ 9.16 (s, 1H), 8.42 (s, 1H), 8.21 (s, 1H), 8.07 (d, J = 1.8 Hz, 1H), 7.95 (d, J = 8.5 Hz, 1H), 7.81 (d, J = 1.4 Hz, 1H), 7.47 (dd, J = 8.5, 2.1 Hz, 1H), 7.39 (d, J = 2.1 Hz, 1H), 3.83 (s, 2H), 2.55 (dd, J = 13.1, 5.5 Hz, 2H), 2.40 (s, 3H), 2.35 (dd, J = 15.2, 7.7 Hz, 2H), 2.21 (s, 6H), 1.78−1.66 (m, 2H). LCMS (FA): m/z 453.2 (M + H).

9-Trifluoromethyl-2-({5-[3-(dimethylamino)propyl]-2-methylpyridin-3-yl}amino)-5,7-dihydro-6H-pyrimido[5,4-d][1]-benzazepine-6-thione (12c). General procedure B using P_2S_5 was used to give **12c** as the formate salt after HPLC purification (4.94 g, 72%). ^{1}H NMR (400 MHz, DMSO) δ 9.23 (s, 1H), 8.47 (s, 1H), 8.19 (s, 1H), 8.14 (d, J = 8.2 Hz, 1H), 8.08 (d, J = 1.8 Hz, 1H), 7.82 (s, 1H), 7.75 (d, J = 8.3 Hz, 1H), 7.68 (s, 1H), 3.87 (s, 2H), 2.55 (dd, J = 14.2, 6.4 Hz, 2H), 2.41 (s, 3H), 2.38 (d, J = 7.7 Hz, 2H), 2.22 (s, 6H), 1.80−1.66 (m, 2H). LCMS (FA): m/z 487.2 (M + H).

Protein Kinase Enzyme Assays. *PLK1 Flash Plate Assay.* The human PLK1 enzymatic reaction totaling 30 μL contained 50 mM Tris-HCl (pH 8.0), 10 mM $MgCl_2$, 0.02% BSA, 10% glycerol, 1 mM DTT, 100 mM NaCl, 3.3% DMSO, 8 μM ATP, 0.2 μCi [γ-^{33}P]-ATP, 4 μM peptide substrate (Biotin-AHX-LDETGHLDSSGLQEVHLA-CONH$_2$), and 10 nM recombinant human PLK1[2−369]T210D. The enzymatic reaction mixture, with or without PLK inhibitors, was incubated for 2.5 h at 30 °C before termination with 20 μL of 150 mM EDTA. Then 25 μL of the stopped enzyme reaction mixture was transferred to a 384-well streptavidin coated Image FlashPlate (Perkin-Elmer) and incubated at room temperature for 3 h. The Image Flash Plate wells were washed three times with 0.02% Tween-20 and then read on the Perkin-Elmer Viewlux.

PLK1 DELFIA Kinase Assay. The human PLK1 enzymatic reaction totaled 30 μL contained 50 mM Tris-HCl (pH 8.0), 10 mM $MgCl_2$, 0.02% BSA, 10% glycerol, 1 mM DTT, 100 mM NaCl, 3.3% DMSO, 50 μM ATP, 2 μM peptide substrate (Biotin-AHX-LDETGHL-DSSGLQEVHLA-CONH$_2$), and 0.3 nM recombinant human PLK1[2−369]T210D. The enzymatic reaction mixture, with or without PLK inhibitors, was incubated 90 min at room temperature before termination with 50 μL of STOP buffer containing 1% BSA, 0.05% Tween 20, 100 mM EDTA. Then 50 μL of the stopped enzyme reaction mixture was transferred to a Neutravidin-coated 384-well plate (Pierce) and incubated at room temperature for 60 min. The wells were washed with wash buffer (25 mM Tris, 150 mM sodium chloride, and 0.1% Tween 20) and incubated for 1 h with 50 μL of antibody reaction mixture containing 1% BSA, 0.05% Tween 20, antiphospho-cdc25c rabbit monoclonal antibody (325 pM, Millennium Pharmaceuticals), and europium labeled antirabbit IgG (2 nM,

Perkin-Elmer). The wells were washed, and then the bound europium was liberated using 50 μL of Enhancement Solution (Perkin-Elmer). Quantification of europium was done using a Pherastar (BMG Labtech)

Cellular Assays. *Cdc25C-T96 Assay.* HeLa cells were seeded in a 96-well cell culture plate (4.5×10^3 cells/well) and incubated overnight at 37 °C. pSGcdc25C (0.05 ug) and pCDNA3.1 PLK T210D (0.02 ug) DNA was transfected using 0.15 mL of Fugene 6 (Roche) transfection reagent in each well. Cells were incubated with PLK1 inhibitors for 2 h at 37 °C, fixed with 4% paraformaldehyde for 15 min, and then permeabilized 15 min with 0.5% Triton X-100 in PBS. Then 100 mL of Roche blocking buffer was added to the wells prior to incubation with rabbit anti-pcdc25c T96 (1:2500, Millennium Pharmaceuticals) and mouse antimyc (clone 9E10) (1:250, Millennium Pharmaceuticals Inc.) antibodies overnight at 4 °C. After washing with PBS, the cells were stained with antirabbit IgG Alexa 488 (1:500, Molecular Probes) and antimouse IgG Alexa 660 (1:500) for 45 min at room temperature. DNA was then stained with Hoechst solution (2 μg/mL). The percentage of pcdc25c and antimyc positive cells were quantified using the Opera instrument and Acapella Image analysis (Perkin-Elmer.)

Mitotic Index Assay. HT29 cells (2.5×10^3 cells/well) in 75 μL of McCoy's 5A media (Invitrogen) supplemented with 10% fetal bovine serum (Invitrogen) was seeded in wells of a 96-well Optilucx plate (BD bioscience) and incubated overnight at 37 °C. Then 25 μL of serially diluted test compounds in McCoy's 5A media supplemented with 10% Fetal Calf Serum (Gibco) were added to the wells. Cells were incubated for 24 h at 37C and then fixed with the addition of 50 μL of 4% paraformaldehyde for 10 min and permeabilized with the addition of 50 μL of 0.5% TritonX-100 in PBS. After washing with PBST, 50 μL of 0.5% Roche blocking buffer was added to the wells and incubated for 1 h at room temperature. Cells were then incubated with mouse anti-pHistone H3 (1:500, Millennium Pharmaceuticals) for 1 h at room temperature. After washing with PBST, the cells were stained with antimouse IgG Alexa 594 (1:200) for 1 h at room temperature. DNA was then stained with Hoechst solution (2 μg/mL). The percentage of pHistone H3 cells were quantified using Discovery-1 and MetaMorph (Molecular Devices.)

Antiproliferation Assays. Eight μL of serially diluted test compounds were added to 75 μL of HT29 (2.66×10^4 cells/well) cells in McCoy's 5A media supplemented with 10% Fetal Calf Serum (Gibco) in Biocoat Poly-D lysine 384 well Black/Clear plates (BD Biosciences). Cells were incubated for 72 h at 37 °C. Supernatant was aspirated from the wells, leaving 25 μL in each well. ATP-lite 1 step reagent (25 μL, Roche) was added to each well, and luminescence for each plate was read on the LeadSeeker (Amersham Biosciences). Percent inhibition was calculated using the values from a DMSO control set to 100%.

In Vivo Studies. *Cell Culture and Tumor Model.* HT29 cells were obtained from ATCC and were cultured in McCoy's 5A medium supplemented with 10% FBS. HT29 cells (2×10^6) were resuspended in Hanks buffer and injected subcutaneously into the flanks of female Nude mice (Taconic). All animals were housed and handled in accordance with the Guide for the Care and Use of Laboratory Animals.

Pharmacokinetics: Sample Harvest and Analysis. All compounds were formulated in a mixture of 2-hydroxypropyl-β-cyclodextrin (HPβCD) (w/w 10%) and dextrose (w/w 2.5%). HT29 tumor bearing animal were dosed orally with compound. At indicated time points, animals were euthanized with CO_2 asphyxiation and cardiac puncture was used to obtain whole blood. Collected blood was quickly transferred into K_2EDTA labeled tubes, centrifuged, and plasma was analyzed for compound concentration. Tumor tissue was surgically removed, weighed, and homogenized in mouse plasma (1:4, equivalent weight in milligrams vs plasma volume in microliters) using a FastPrep-24 homogenizer (MP Biomedicals, Solon, OH) for concentration analysis. The quantification of compound was conducted by a method based on a liquid chromatography tandem mass spectrometry (LC/MS/MS) methodology. Compound was extracted from the protein matrix by precipitating the proteins in samples with

acetonitrile at a ratio of 1:4 (v/v, sample/acetonitrile). The internal standard used for analysis was a stable isotope labeled MLN0905. The dynamic range of the assay was 1−1000 nM. The pharmacokinetic analysis was performed using Winonlin software (Pharsight, St. Louis, Missouri).

Immunohistochemistry. HT29 tumor bearing mice were dosed orally with compound and at indicated time points tumor tissue harvested and placed in 10% neutral buffered formalin. Immunofluoresence was performed on 5 μm of paraffin embedded tumor sections using the Discovery XT automated staining system (Ventana Medical Systems, Tucson, AZ). Sections were deparaffinized, followed by epitope unmasking with cell conditioning 1 solution (Ventana Medical Systems) for 20 min. Tumor sections were stained for pHisH3 (Cell Signaling Technologies, Danvers, MA). The deoxyribonucleic acid (DNA) stain 4′,6-diamidino-2-phenylindole (DAPI, Vector Laboratories, Inc., Burlingame, CA) was used to estimate the total number of cells/field. One tissue section was used for each of the three animals in a treatment group. Images were acquired using a Leica DMLB microscope (Leica Microsystems, Wetzlar, Germany) with a Photometrics Cool Snap HQ Nikon Eclipse E800 camera. Five images from each slide were captured using a 20× Leica Plan objective (Leica Microsystems, Wetzlar Germany) and analyzed on Metamorph 6.3r7 image processing software (Molecular Devices, Downingtown, PA) using a custom image processing application module (Molecular Devices Inc., City, State). The number of pHisH3-positive cells were counted and averaged in the five fields of view, and DAPI Vectashield HardSet Medium (Vector Laboratories, Burlingame, CA) was used as a chromatin counter stain.

Efficacy Studies. Tumor growth was monitored using vernier calipers, and the mean tumor volume was calculated using the formula $V = W^2 \times L/2$. When the mean tumor volume reached approximately 200 mm^3, the animals were randomized into treatment groups ($n = 10$ animals/group). Tumor growth and body weights were measured twice per week.

In Vivo Statistical Analysis. *Treatment over Control (T/C).* The mean volume on day x for the treatment group was divided by the mean volume for the control group on day x.

Area under the Tumor Growth Curve (AUC) Analysis (during Treatment). The differences in the tumor growth trends (tumor volume or photon flux) over time between pairs of groups were assessed using linear mixed effects regression models. To compare pairs of groups, the following mixed-effects linear regression model was fit to the data using the maximum likelihood method:

$$Y_{ijk} - Y_{i0k} = Y_{i0k} + \text{treat}_i + \text{day}_i + \text{day}_j + \text{day}_j^2$$
$$+ (\text{treat} \times \text{day})_{ij} + (\text{treat} \times \text{day}^2)_{ij} + \varepsilon_{ijk}$$

where Y_{ijk} is the log$_{10}$ tumor value at the jth time point of the kth animal in the ith treatment, Y_{i0k} is the day 0 (baseline) log$_{10}$ tumor value in the kth animal in the ith treatment, day$_j$ was the median-centered time point and (along with day$_j^2$) was treated as a continuous variable, and ε_{ijk} is the residual error. A spatial power law covariance matrix was used to account for the repeated measurements on the same animal over time. Interaction terms as well as day$_j^2$ terms were removed if they were not statistically significant. A likelihood ratio test was used to assess whether a given pair of treatment groups exhibited differences which were statistically significant. The −2 log likelihood of the full model was compared to one without any treatment terms (reduced model) and the difference in the values were tested using a χ-squared test. The degrees of freedom of the test were calculated as the difference between the degrees of freedom of the full model and that of the reduced model. The predicted differences in the log tumor values ($Y_{ijk} - Y_{i0k}$, which can be interpreted as log$_{10}$ (fold change from day 0)) were taken from the above models to calculate mean AUC values for each treatment group. A dAUC

value was then calculated as:

$$d\text{AUC} = \frac{\text{mean}(\text{AUC}_{\text{ctl}}) - \text{mean}(\text{AUC}_{\text{trt}})}{\text{mean}(\text{AUC}_{\text{ctl}})} \times 100$$

This assumes AUC$_{\text{ctl}}$ was positive. In instances where AUC$_{\text{ctl}}$ was negative, the above formula was multiplied by −1. All P values <0.05 in these analyses were considered statistically significant.

■ ASSOCIATED CONTENT

Ⓢ Supporting Information

Synthetic details and characterization data for all compounds reported in this manuscript are described in full. In addition, crystallographic methods for the crystal structure of **12b** are also available. This material is available free of charge via the Internet at http://pubs.acs.org.

Accession Codes

PDB:ID: Figure 2 crystal structure, **12b** in PLK1, 3THB.

■ AUTHOR INFORMATION

Corresponding Author

*Phone: 617-551-7832. E-mail: matthew.duffey@mpi.com.

■ ACKNOWLEDGMENTS

■ ABBREVIATIONS USED

PLK1, Polo-like kinase 1; shRNA, short hairpin RNA; SAR, structure−activity relationship; HT29, human colon adenocarcinoma grade II cell line; MIA, mitotic index assay; Cdc25C, Cell division cycle 25 homologue C; pH3, phosphohistone H3; HPβCD, (2-hydroxypropyl)-β-cyclodextrin; RNAi, RNA interference; V_{SS}, steady state volume of distribution; CL$_{\text{P}}$, plasma clearance; C_{max}, maximum concentration in plasma; T_{max}, time of measurement of C_{max}; %F, percent bioavailability; $t_{1/2}$, elimination half-life; MTD, maximum tolerated dose; QD, daily

■ REFERENCES

(1) Barr, F. A.; Sillje, H. H. W.; Nigg, E. A. Polo-like kinases and the orchestration of cell division. *Nature Rev. Mol. Cell. Biol.* **2004**, *5*, 429−441.

(2) (a) Kneisel, L.; Strebhardt, K.; Bernd, A.; Wolter, M.; Binder, A.; Kaufmann, R. Expression of polo-like kinase (PLK1) in thin melanomas: a novel marker of metastatic disease. *J. Cutaneous Pathol.* **2002**, *29*, 354−358. (b) Takai, N.; Miyazaki, T.; Fujisawa, K.; Nasu, K.; Hamanaka, R.; Miyakawa, I. Polo-like kinase (PLK) expression in endometrial carcinoma. *Cancer Lett.* **2001**, *164*, 41−49. (c) Takahashi, T.; Sano, B.; Nagata, T.; Kato, H.; Sugiyama, Y.; Kunieda, K.; Kimura, M.; Okano, Y.; Saji, S. Polo-like kinase 1 (PLK1) is overexpressed in primary colorectal cancers. *Cancer Sci.* **2003**, *94*, 148−152. (d) Macmillan, J. C.; Hudson, J. W.; Bull, S.; Dennis, J. W.; Swallow, C. J. Comparative expression of the mitotic regulators SAK and PLK in colorectal cancer. *Ann. Surg. Oncol.* **2001**, *8*, 729−740. (e) Gray, P. J.; Bearss, D. J.; Han, H.; Nagle, R.; Tsao, M.-S.; Dean, N.; Von Hoff, D. D. Identification of human polo-like kinase 1 as a potential therapeutic target in pancreatic cancer. *Mol. Cancer. Ther.* **2004**, *3*, 641−646. (f) Dietzmann, K.; Kirches, E.; von Bossanyi, P.; Jachau, K.; Mawrin, C. Increased human polo-like kinase-1 expression in gliomas. *J. Neurooncol.* **2001**, *53*, 1−11. (g) Ito, Y.; Miyoshi, E.;

Sasaki, N.; Kakudo, K.; Yoshida, H.; Tomoda, C.; Uruno, T.; Takamura, Y.; Miya, A.; Kobayashi, K.; Matsuzuka, F.; Matsuura, N.; Kuma, K.; Miyauchi, A. Polo-like kinase 1 overexpression is an early event in the progression of papillary carcinoma. *Br. J. Cancer* **2004**, *90*, 414−418. (h) Weichert, W.; Schmidt, M.; Jacob, J.; Gekeler, V.; Langrehr, J.; Neuhaus, P.; Bahra, M.; Denkert, C.; Dietel, M.; Kristiansen, G. Overexpression of Polo-Like Kinase 1 Is a Common and Early Event in Pancreatic Cancer. *Pancreatology* **2005**, *5*, 259−265. (i) Mito, K.; Kashima, K.; Kikuchi, H.; Daa, T.; Nakayama, I.; Yokoyama, S. Expression of Polo-Like Kinase (PLK1) in Non-Hodgkin's Lymphomas. *Leuk. Lymphoma* **2005**, *46*, 225−231. (j) Liu, L.; Zhang, M.; Zou, P. Polo-like kinase 1 as a new target for non-Hodgkin's lymphoma treatment. *Oncology* **2008**, *74*, 96−103. (k) Yamamoto, Y.; Matsuyama, H.; Kawauchi, S.; Matsumoto, H.; Nagao, K.; Ohmi, C.; Sakano, S.; Furuya, T.; Oga, A.; Naito, K.; Sasaki, K. Overexpression of Polo-Like Kinase 1 (PLK1) and Chromosomal Instability in Bladder Cancer. *Oncology* **2006**, *70*, 231−237. (l) Weichert, W.; Ullrich, A.; Schmidt, M.; Gekeler, V.; Noske, A.; Niesporek, S.; Buckendahl, A.-C.; Dietel, M.; Denkert, C. Expression patterns of polo-like kinase 1 in human gastric cancer. *Cancer Sci.* **2006**, *97*, 271−276.

(3) Wolf, G.; Elez, R.; Doermer, A.; Holtrich, U.; Ackermann, H.; Stutte, H. J.; Altmannsberger, H.-M.; Rübsamen-Waigmann, H.; Strebhardt, K. Prognostic significance of polo-like kinase (PLK) expression in non-small cell lung cancer. *Oncogene* **1997**, *14*, 543−549. (b) Knecht, R.; Elez, R.; Oechler, M.; Solbach, C.; von Ilberg, C.; Strebhardt, K. Prognostic Significance of *Polo-like Kinase (PLK)* Expression in Squamous Cell Carcinomas of the Head and Neck. *Cancer Res.* **1999**, *59*, 2794−2797. (c) Strebhardt, K.; Kneisel, L.; Linhart, C.; Bernd, A.; Kaufmann, R. Prognostic value of pololike kinase expression in melanomas. *JAMA, J. Am. Med. Assoc.* **2000**, *283*, 479−480. (d) Weichert, W.; Kristiansen, G.; Schmidt, M.; Gekeler, V.; Noske, A.; Niesporek, S.; Dietel, M.; Denkert, C. Polo-like kinase 1 expression is a prognostic factor in human colon cancer. *World J. Gastroenterol.* **2005**, *11*, 5644−5650. (e) Tokumitsu, Y.; Mori, M.; Tanaka, S.; Akazawa, K.; Nakano, S.; Niho, Y. Prognostic significance of polo-like kinase expression in esophageal carcinoma. *Int. J. Oncol.* **1999**, *15*, 687−692. (f) Weichert, W.; Schmidt, M.; Gekeler, V.; Denkert, C.; Stephan, C.; Jung, K.; Loening, S.; Dietel, M.; Kristiansen, G. Polo-like kinase 1 is overexpressed in prostate cancer and linked to higher tumor grades. *Prostate* **2004**, *60*, 240−245. (g) Kanaji, S.; Saito, H.; Tsujitani, S.; Matsumoto, S.; Tatebe, S.; Kondo, A.; Ozaki, M.; Ito, H.; Ikeguchi, M. Expression of polo-like kinase 1 (PLK1) protein predicts the survival of patients with gastric carcinoma. *Oncology* **2006**, *70*, 126−133.

(4) Smith, M. R.; Wilson, M. L.; Hamanaka, R.; Chase, D.; Kung, H.; Longo, D. L.; Ferris, D. K. Malignant transformation of mammalian cells initiated by constitutive expression of the polo-like kinase. *Biochem. Biophys. Res. Commun.* **1997**, *234*, 397−405.

(5) (a) Spänkuch-Schmitt, B.; Bereiter-Hahn, J.; Kaufmann, M.; Strebhardt, K. Effect of RNA silencing of polo-like kinase-1 (PLK1) on apoptosis and spindle formation in human cancer cells. *J. Natl. Cancer Inst.* **2002**, *94*, 1863−1877. (b) Spänkuch-Schmitt, B.; Wolf, G.; Solbach, C.; Loibl, S.; Knecht, R.; Stegmüller, M.; von Minckwitz, G.; Kaufmann, M.; Strebhardt, K. Downregulation of human polo-like kinase activity by antisense oligonucleotides induces growth inhibition in cancer cells. *Oncogene* **2002**, *21*, 3162−3171.

(6) Liu, X.; Lei, M.; Erikson, R. L. Normal cells, but not cancer cells, survive severe Plk1 depletion. *Mol. Cell. Biol.* **2006**, *26*, 2093−2108.

(7) Spänkuch, B; Matthess, Y; Knecht, R; Zimmer, B; Kaufmann, M; Strebhardt, K. Cancer inhibition in nude mice after systemic application of U6 promoter-driven short hairpin RNAs against PLK1. *J. Natl. Cancer Inst* **2004**, *96*, 862−872.

(8) (a) Schoffski, D. Polo-like kinase (PLK) inhibitors in preclinical and early clinical development in oncology. *Oncologist* **2009**, *14*, 559−570. (b) Christoph, D. C.; Schuler, M. Polo-like kinase 1 inhibitors in mono- and combination therapies: a new strategy for treating malignancies. *Expert Rev. Anticancer Ther.* **2011**, *11*, 1115−1130.

(9) Solubility in this study was determined by a turbidimetric solubility assay which provides the kinetic solubility of compounds in 50 mM potassium phosphate buffer at pH 6.8. Our target for an acceptable solubility profile was 100 mg/mL in this assay.

(10) While the 9-iodo (**5a**) and 9-trifluoromethyl (**5b**) analogues of **1** did show slight improvements in enzyme activity, these differences in activity were minimal. We chose to create analogues with the 9-chloro substituent because of better accessibility to starting material, and we were confident that after optimization of the upper aryl ring we would be able to survey chloride replacements for a fully optimized scaffold.

(11) Huang, X.; Anderson, K. W.; Zim, D.; Jiang, L.; Klapars, A.; Buchwald, S. L. Expanding Pd-Catalyzed C−N Bond-Forming Processes: The First Amidation of Aryl Sulfonates, Aqueous Amination, and Complementarity with Cu-Catalyzed Reactions. *J. Am. Chem. Soc.* **2003**, *125*, 6653−6655.

(12) The MIA screens small molecule inhibitors of human PLK. The inhibition of PLK results in cell cycle arrest in pro-metaphase, which is detected by a phospho-histone H3 (ser10) monoclonal antibody (pH3). This IF assay measures an EC_{30} or accumulation of 30% positive pH3 in cells.

(13) Toyoshima-Morimoto, F.; Toyoshima-Morimoto, E.; Nishida, E. Plk1 promotes nuclear translocation of human Cdc25C during prophase. *EMBO Rep.* **2002**, *3*, 341−348.

(14) Kothe, M.; Kohls, D.; Low, S.; Coli, R.; Cheng, A. C.; Jacques, S. L.; Johnson, T. L.; Lewis, C.; Loh, C.; Nonomiya, J.; Sheils, A. L.; Verdries, K. A.; Wynn, T. A.; Kuhn, C.; Ding, Y.-H. Structure of the Catalytic Domain of Human Polo-like Kinase 1. *Biochemistry* **2007**, *46*, 5960−5971.

(15) (a) Kothe, M.; Kohls, D.; Low, S.; Coli, R.; Rennie, G. R.; Feru, F.; Kuhn, C.; Ding, Y. Selectivity-determining Residues in Plk1. *Chem. Biol. Drug Des.* **2007**, *70*, 540−546. (b) Beria, I.; Ballinari, D.; Bertrand, J. A.; Borghi, D.; Bossi, R. T.; Brasca, M. G.; Cappella, P.; Caruso, M.; Ceccarelli, W.; Ciacolella, A.; Cristiani, C.; Croci, V.; De Ponti, A.; Fachin, G.; Ferguson, R. D.; Lansen, J.; Moll, J. K.; Pesenti, E.; Posteri, H.; Perego, R.; Rocchetti, M.; Storici, P.; Volpi, D.; Valsasina, B. Identification of 4,5-Dihydro-1*H*-pyrazolo[4,3-*h*]quinazoline Derivatives as a New Class of Orally and Selective Polo-Like Kinase 1 Inhibitors. *J. Med. Chem.* **2010**, *53*, 3532−3551.

(16) Beria, I.; Valsasina, B.; Brasca, M. G.; Ceccarelli, W.; Colombo, M.; Cribioli, S.; Fachin, G.; Ferguson, R. D.; Fiorentini, F.; Gianellini, L. M.; Giorgini, M. L.; Moll, J. K.; Posteri, H.; Pezzetta, D.; Roletto, F.; Sola, F.; Tesei, D.; Caruso, M. 4,5-Dihydro-1*H*-pyrazolo[4,3-*h*]-quinazolines as potent and selective Polo-like kinase 1 (PLK1) inhibitors. *Bioorg. Med. Chem. Lett.* **2011**, *21*, 2969−2974.

(17) Bharathan, I.; Duffey, M. O.; Elder, A. M.; Guo, J.; Li, G.; Reynolds, D.; Soucy, F.; Vos, T. J. 5,7-Dihydro-6*H*-pyrimido[5,4-*d*][1]-benzazepin-6-thiones as PLK inhibitors. Patent WO 2010/065134 A1, 2010.

(18) Additional kinase binding data for **12b** and **12c** can be found in Supporting Information Tables 1 and 2.

(19) Degenhardt, Y.; Lampkin, T. Targeting Polo-like kinase in cancer therapy. *Clin. Cancer Res.* **2010**, *16*, 384−389.

(20) (a) Scutt, P. J.; Chu, M. L. H.; Sloane, D. A.; Cherry, M.; Bignell, C. R.; Williams, D. H.; Eyers, P. A. Discovery and Exploitation of Inhibitor-Resistant Aurora and Polo Kinase Mutants for the Analysis of Mitotic Networks. *J. Biol. Chem.* **2009**, *284*, 15880−15893. (b) Steegmaier, M.; Hoffmann, M.; Baum, A.; Lénárt, P.; Petronczki, M.; Krssák, M.; Gürtler, U.; Garin-Chesa, P.; Lieb, S.; Quant, J.; Grauert, M.; Adolf, G. R.; Kraut, N.; Peters, J. M.; Rettig, W. J. BI 2536, A Potent and Selective Inhibitor of Polo-like Kinase 1, Inhibits Tumor Growth in Vivo. *Curr. Biol.* **2007**, *17*, 316−322.

(21) (a) Gilmartin, A. G.; Bleam, M. R.; Richter, M. C.; Erskine, S. G.; Kruger, R. G.; Madden, L.; Hassler, D. F.; Smith, G. K.; Gontarek, R. R.; Courtney, M. P.; Sutton, D.; Diamond, M. A.; Jackson, J. R.; Laquerre, S. G. Distinct Concentration-Dependent Effects of the Polo-like Kinase 1-Specific Inhibitor GSK461364A, Including Differential Effect on Apoptosis. *Cancer Res.* **2009**, *69*, 6969−6877.